RESEARCH ARTICLE | JULY 01 1972

Mechanism by Which a Two-Dimensional Roughness Element Induces Boundary-Layer Transition

P. S. Klebanoff; K. D. Tidstrom

Physics of Fluids 15, 1173–1188 (1972)
https://doi.org/10.1063/1.1694065

Mechanism by Which a Two-Dimensional Roughness Element Induces Boundary-Layer Transition

P. S. KLEBANOFF AND K. D. TIDSTROM
National Bureau of Standards, Washington, D. C. 20234

(Received 15 December 1971; final manuscript received 24 February 1972)

An experimental investigation of the effect of two-dimensional roughness elements on boundary-layer transition is described. Primary emphasis is given to the nature of disturbances within the recovery zone, i.e., that region in the immediate downstream of the roughness where the mean flow has been distorted by the presence of the roughness. Detailed measurements of mean velocity distributions, of disturbance spectra, and intensity, growth, and decay of disturbances at discrete frequencies were made for a range of unit Reynolds numbers. The measurements demonstrate that the behavior can best be understood by considering wave-type disturbances, and that the basic mechanism by which a two-dimensional roughness element induces earlier transition to turbulent flow is by the destabilizing influence of the flow within the recovery zone. Comparison with the behavior expected from stability theory supports this conclusion.

I. INTRODUCTION

The transition from laminar to turbulent flow in boundary layers is a phenomenon of great importance in those aspects of our technology involving the flow of gases or liquids. Consequently, it has been a subject of active research for many years. The major experimental effort has been made in aerodynamics not only because it has been experimentally convenient but more importantly because of the very strong influence boundary-layer transition has on many aerodynamic characteristics, and the extrapolation of test data to actual conditions. This extensive effort has been rewarding in that considerable progress has been made in our understanding of the fundamental processes. However, a reliable method for predicting transition in practical applications is still not available. Apart from the inherent complexities of the phenomenon the difficulties are compounded by the many factors which affect transition, such as surface temperature, surface curvature, pressure gradients, free-stream disturbances, surface roughness, etc. The interest in laminar-flow airfoils, as well as the desirability, in some situations, of tripping the boundary layer to make it turbulent has focused a great deal of attention on the effect of surface roughness. There has been considerable experimental activity dealing with the effect of both two- and three-dimensional roughness elements on the transition from laminar to turbulent flow in boundary layers at subsonic, supersonic, and even hypersonic speeds.

The effect of surface roughness is to induce earlier transition; that is, to move the position on the surface where transition occurs upstream relative to where it would be without the roughness. For a given two-dimensional roughness element the change in transition position is a gradual one with increasing velocity. For a three-dimensional roughness element the behavior is somewhat more critical in nature, with transition moving rapidly forward to the roughness with a relatively small increase in velocity after a critical velocity has been reached. This, simply stated, describes the observed phenomenological behavior of discrete roughness elements except to say that it appears to be much more difficult to trip the boundary layer at the higher Mach numbers.

The approach to date has been empirical and limited to obtaining what may be termed design data. It has concerned itself with correlating the position of transition with the various pertinent parameters suggested by dimensional analysis and a number of interesting empirical correlations have been obtained. Reynolds numbers have been determined for when roughness does not affect transition, and for when transition is attached to the roughness. Correlations of the Reynolds number of transition have also been determined with roughness size and position, and boundary-layer thickness. It is not meant to minimize the importance or usefulness of these results but it is felt that this approach, as in the case of much of the earlier work on transition, reflects only indirectly the mechanism by which roughness affects transition, and has reached the point of diminishing return as far as an understanding of the basic mechanism is concerned. Although there have been some isolated inferences in the literature[1–4] that the behavior of roughness elements is due to a modification of the stability characteristics of the flow, this point of view has not been pursued. Our knowledge to date as to the basic mechanism has been covered by the heuristic argument that in some vague, unspecified manner the roughness introduces disturbances which raise the disturbance level. It is particularly in this area that there has been a lack of definitive experimental information. It was with the purpose of providing information on this aspect that the present investigation was undertaken. The effort reported on herein is confined to the study of single two-dimensional roughness elements and is directed toward gaining an insight into the basic mechanism by which such roughness elements affect transition.

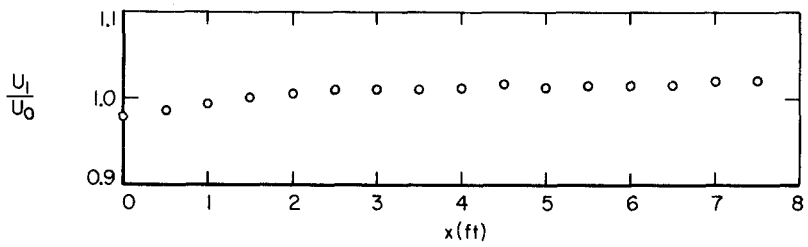

FIG. 1. Distribution of free-stream velocity along flat plate at $U_0/\nu = 1.42\times10^5$ (ft^{-1}).

II. EXPERIMENTAL ARRANGEMENT AND PROCEDURE

The investigation was carried out using a boundary layer on an aluminum plate, 12 ft long, $4\frac{1}{2}$ ft wide and $\frac{1}{4}$ in. thick which had a symmetrically tapered and sharpened leading edge. It was mounted vertically and centrally in the National Bureau of Standards $4\frac{1}{2}$ ft wind tunnel. A false wall mounted on the tunnel wall facing the working side of the plate permitted the adjustment of the pressure gradient within moderate limits and was used to compensate for the boundary-layer growth. A positive angle of attack was obtained by displacing the leading edge slightly and by some blocking of the air passage on the working side at the downstream end of the plate. This was done in order to have the stagnation point on the working side of the plate, and to have smooth flow conditions at the leading edge. The distribution of mean velocity, U_1, in the free stream outside the boundary layer, with distance from the leading edge, x, is shown in Fig. 1. U_0 is the mean velocity of the flow approaching the plate, used as a reference velocity.

Two-dimensional roughness elements in the form of cylindrical rods, 3 ft long, were used. They were attached to the surface by adhesion to a double-sided adhesive strip applied to the surface. The roughness element spanned the plate for a distance of 18 in. on each side of the centerline. Except as noted, the investigation, for the most part, was carried out using a cylindrical rod $\frac{1}{16}$ in. diameter attached to the surface at a distance x_k, 2 ft from the leading edge. The actual roughness height k, that resulted from the method of attachment was 0.066 in. Subsequent reference to roughness size refers to the actual roughness height which was used in all cases.

Primary emphasis was placed on the nature of the disturbances within the recovery zone. The recovery zone is defined here as the region in the downstream vicinity of the roughness where the mean flow has been distorted by the presence of the roughness. More explicitly, it is the region between the roughness element and the recovery position, where the recovery position is the downstream position at which the mean velocity profile has returned to the type of distribution that it would have without the roughness. Figure 2 shows the distribution of the x component of local mean velocity U, in the boundary layer with distance from the surface y at several positions along the plate without roughness. The distributions are plotted nondimensionally, ν being the kinematic viscosity, for comparison with the Blasius distribution. The measurements shown were made at a unit Reynolds number U_0/ν, of 1.42×10^5(ft^{-1}); however, no significant variation in the nature of the distributions shown in Figs. 1 and 2 was observed over the range of unit Reynolds numbers covered in this investigation. The displacement of the leading edge, and the associated favorable pressure gradient existing over the forward part of the plate, resulted in a velocity distribution 2 ft from the leading edge that has a displacement thickness which is 0.94 of the Blasius value, but within the experimental uncertainty, the profile shape is still of the Blasius type when compared on a y/δ^* basis.

It is customary to correlate transition data for two-dimensional roughness elements in a zero-pressure gradient boundary layer with the parameter k/δ_k^*, where δ_k^* is the boundary-layer displacement thickness at the roughness position without the roughness present. Although, at 2 ft from the leading edge the measured δ_k^* is less than the Blasius value,

$$\delta_k^* = 1.72(\nu x_k/U_1)^{1/2},$$

the Blasius value is used in presenting the data for roughness elements at this position. At positions 3 ft

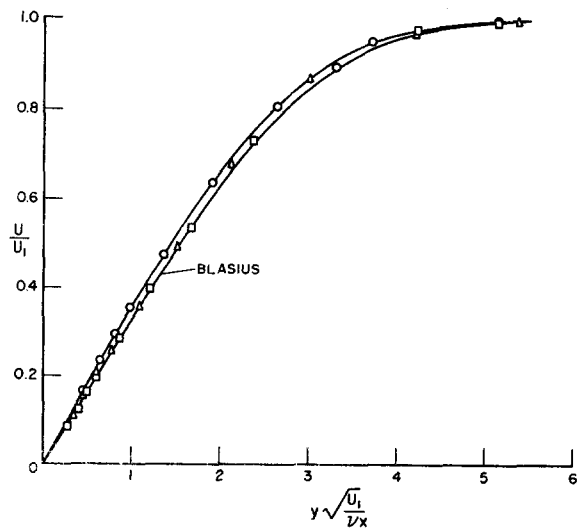

FIG. 2. Mean-velocity distributions at various positions along flat plate without roughness at $U_0/\nu = 1.42\times10^5$ (ft^{-1}). ⊙ $x=2$ ft, △ $x=3$ ft, ⊡ $x=5$ ft.

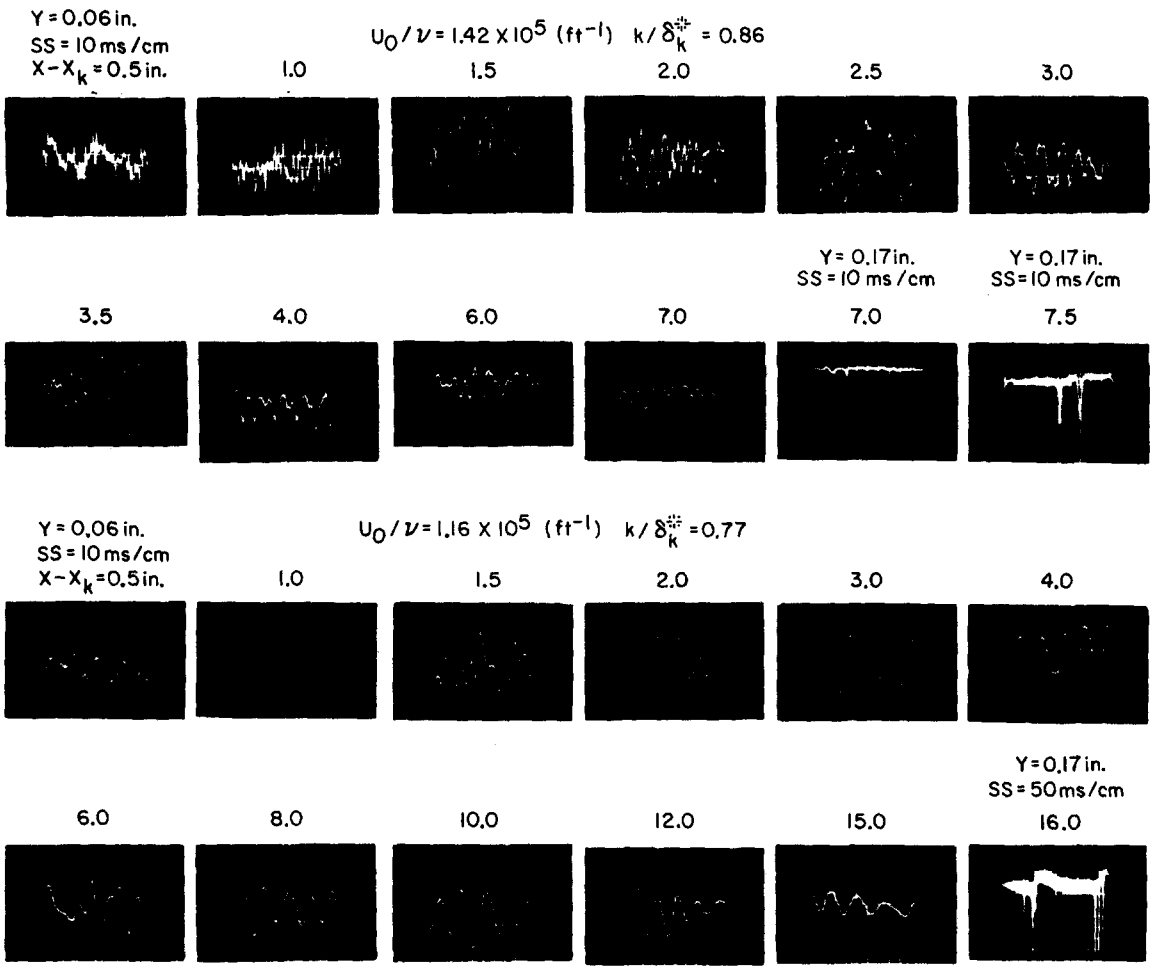

FIG. 3. Oscillograms of u fluctuation downstream of 0.066-in. diam. roughness element at $x = 2.0$ ft. Decreasing velocity is in downward direction. Time is increasing from left to right.

from the leading edge, and farther downstream the measured values are in good agreement with the Blasius value. As shown in Sec. IV there is an upstream influence of the roughness, and at approximately 30 roughness diameters upstream the mean velocity profile still does not exhibit the undisturbed profile expected from Fig. 2, in fact, it approximates a Blasius profile fairly well. The use of a δ_k^* as such would therefore seem somewhat arbitrary and nebulous. The Blasius value, on the other hand, implies a realizable length scale, proportional to $(\nu x_k/U_1)^{1/2}$, with the roughness present, and provides consistency with other investigations.

Measurements of intensity, spectra, growth and decay of velocity fluctuations at discrete frequencies, as well as mean velocity distributions were made over a range of unit Reynolds numbers using conventional constant-current hot-wire anemometry. For spectral measurements, and the growth and decay at discrete frequencies, a wave analyzer having a fixed bandpass with an effective bandwidth of 4.8 Hz was used. The measurements were confined to the longitudinal components of the velocity fluctuation and of the mean velocity. Platinum wires 0.0001 in. diam, ranging in length from 0.02–0.04 in., were used and no correction for wire length, nor for the nonlinear response of the hot wire, was deemed necessary. Film recordings of the fluctuation from a cathode-ray oscilloscope also proved useful.

At a unit Reynolds number per ft of $3\times10^5(\text{ft}^{-1})$ the beginning of transition on the plate without roughness occurred at about 9.5 ft from the leading edge. No significant spanwise variations in the mean velocity were observed in the boundary layer on the flat plate without roughness. However, spanwise variations in intensity of the disturbances were observed downstream of the roughness. These were particularly pronounced at the higher Reynolds numbers where transition was fairly close to the roughness, and the transition region was relatively short indicating that transition in this case was relatively better fixed. The measurements presented herein were made, therefore, at a

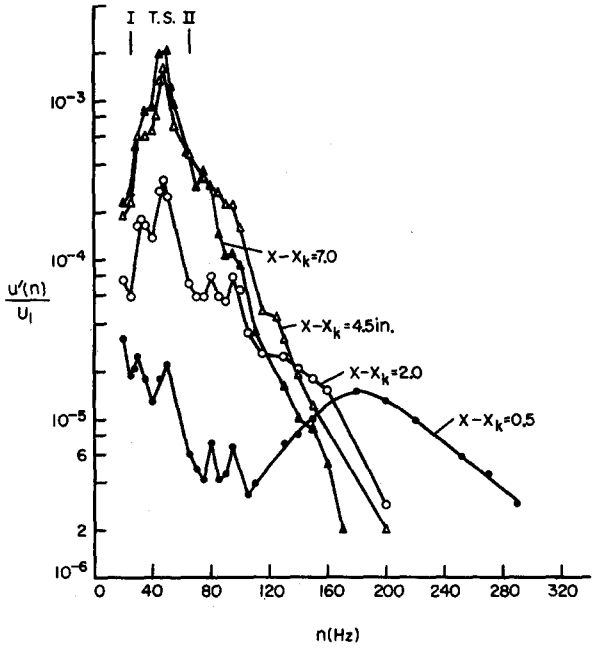

FIG. 4. Spectra of u fluctuation downstream of 0.066-in. diam roughness element at $x_k=2.0$ ft, $U_0/\nu=1.16\times10^5$ (ft^{-1}), $y=0.06$ in.

spanwise position corresponding to a peak in the spanwise distribution of intensity of disturbances. This position remained fixed in the downstream direction.

III. DISTURBANCES

Oscillograms of the longitudinal component of the velocity fluctuation u, in the boundary layer at Reynolds numbers per ft of 1.16×10^5 and 1.42×10^5 are shown in Fig. 3. The corresponding values of k/δ_k^*, a parameter commonly used in correlating empirical data on Reynolds numbers of transition, are noted in the figure. The different distances downstream from the rod are noted above each oscillogram, and in each case the hot wire was at 0.06 in. from the surface except for the oscillograms which illustrate breakdown which were obtained farther out in the boundary layer, at 0.17 in. from the surface, where the "breakdown" process is more readily observed. It is seen that the "spikes" which characterize the "breakdown" process[5,6] do occur; however, they now occur intermittently in contrast to previous observations of the "spike" in experiments using the vibrating ribbon which afforded a well-controlled perturbation. The reciprocal sweep speed was 10 msec/cm for each of the oscillograms except for the oscillogram which illustrates "breakdown" at the lower unit Reynolds number, where the reciprocal sweep speed was 50 msec/cm. There is no significant reason for this other than the fact that at the lower unit Reynolds number the transition region is of much greater extent than at the higher unit Reynolds number, about 3 ft as compared with 1 ft with "breakdown" being a great deal more sporadic, and the slower sweep speed enhanced the period of observation. No significance should be attached to the relative amplitudes of the fluctuations shown in the different oscillograms. The amplifier gain, as well as the wire sensitivity, varied and the amplitudes are not shown in true proportion to one another.

In a qualitative way these oscillograms are very informative. They reinforce the view that downstream of a two-dimensional roughness element transition occurs in the same manner as it does on a smooth plate. They indicate that upstream of breakdown highly concentrated discrete vortices are not present. At the lower Reynolds number, close to the rod, it is seen that the fluctuation is composed of relatively higher frequencies and in a downstream direction there is a continuous change to lower and lower frequencies, and in this case, there emerges a relatively pure frequency of about 50 Hz with a time-varying amplitude. The same behavior is observed at the higher Reynolds number except that at each comparable downstream position the fluctuation is composed of higher frequencies. If discrete vortices were present, one would expect to observe the same frequency at each downstream position, and it is difficult to reconcile the existence of discrete vortices with the continuous variation in the frequency content. A more reasonable explanation is that there is a wave selection process within the recovery zone in the manner one would expect from stability theory.

This behavior is illustrated in more detail and in a more quantitative manner in Fig. 4 which shows the spectral distribution at different distances downstream from the roughness at a unit Reynolds number of 1.16×10^5(ft^{-1}). A semilog plot was used because of the large scale that is required. The measurements were made 0.06 in. from the surface, and instead of the customary power spectrum, the spectra are presented in terms of the intensity, where $u'(n)$ is the rms value of u associated with the frequency n. The distance of the beginning of transition from the leading edge x_t, was determined by observations of the beginning of turbulent bursts with a hot wire near the surface with an uncertainty of ±1 in. This position was, in general, a few inches farther downstream from the position where the "spikes" were first observed to occur, and at a unit Reynolds number of 1.16×10^5(ft^{-1}), was 19 in. downstream from the roughness. The two vertical lines at the top of the figure are the frequencies corresponding to branch I and branch II of the Tollmien–Schlichting stability diagram as calculated by Shen,[7] and as determined from the boundary-layer Reynolds number at the recovery position. The recovery position, as will be shown in Sec. IV, is taken to be at 4.5 in. from the roughness element. The sharp peaks in the variation of intensity with frequency 0.5 in. downstream from the roughness are due to the wind tunnel disturbances. They correlate well with the peaks observed in the

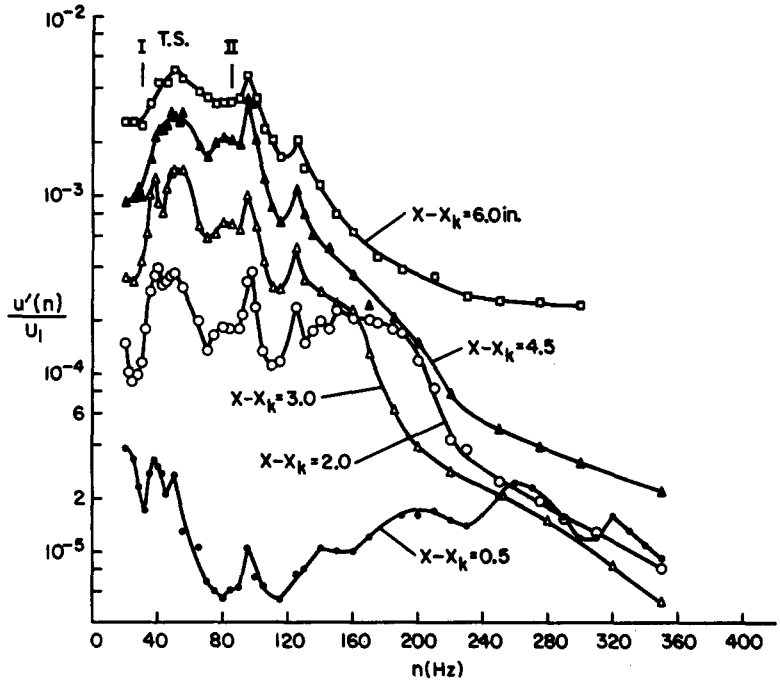

FIG. 5. Spectra of u fluctuation downstream of 0.066-in. diam roughness element at $x_k=2.0$ ft, $U_0/\nu=1.42\times 10^6$ (ft^{-1}), $y=0.06$ in.

wind tunnel noise spectrum as well as with the peaks in the spectrum of the free-stream turbulence. The significant feature is the presence of comparable intensities which lie outside the zone of amplification of the Tollmien–Schlichting stability theory with a maximum at about 180 Hz. It is the contribution of this band of frequencies which is responsible for the higher frequencies referred to earlier in the oscillograms obtained close to the rod. In a downstream direction these higher frequencies damp and the dominant frequency which emerges lies within the Tollmien–Schlichting zone of instability. However, the amplification within the recovery zone is many times greater than the Tollmien–Schlichting amplification as can be seen from the change in amplitude downstream of the recovery position, that is, from 4.5 to 7.0 in. as compared with the change in amplitude from 0.5 to 2.0 in.

Similar spectral distributions are shown in Fig. 5 for a higher unit Reynolds number of 1.42×10^6(ft^{-1})

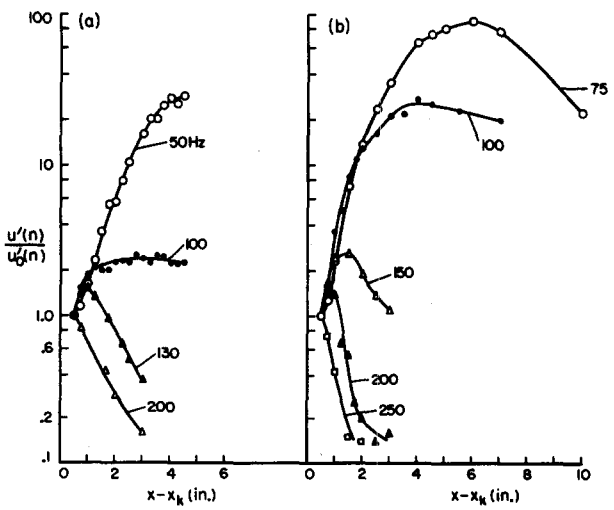

FIG. 6. Growth and decay of various frequencies downstream of 0.066-in. diam roughness element at $x_k=2.0$ ft, $y=0.06$ in. (a) $U_0/\nu=1.0\times 10^6$ (ft^{-1}); (b) $U_0/\nu=1.16\times 10^6$ (ft^{-1}).

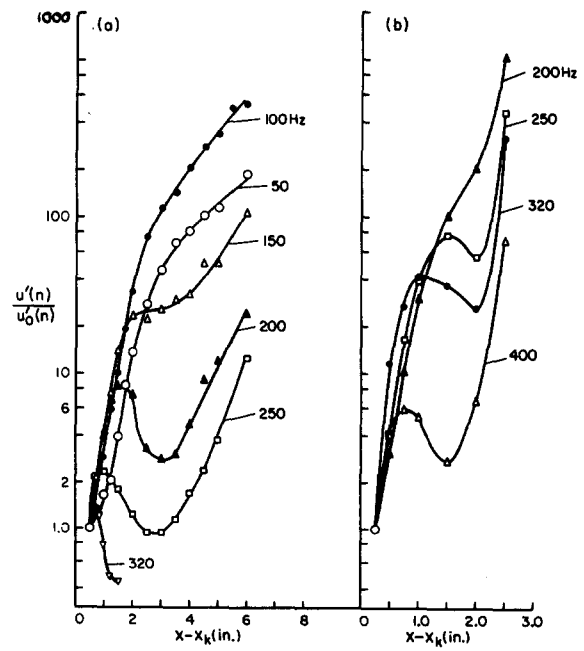

FIG. 7. Growth and decay of various frequencies downstream of 0.066-in. diam roughness element at $x_k=2.0$ ft, $y=0.06$ in.; (a) $U_0/\nu=1.42\times 10^6$ (ft^{-1}); (b) $U_0/\nu=1.67\times 10^6$ (ft^{-1}).

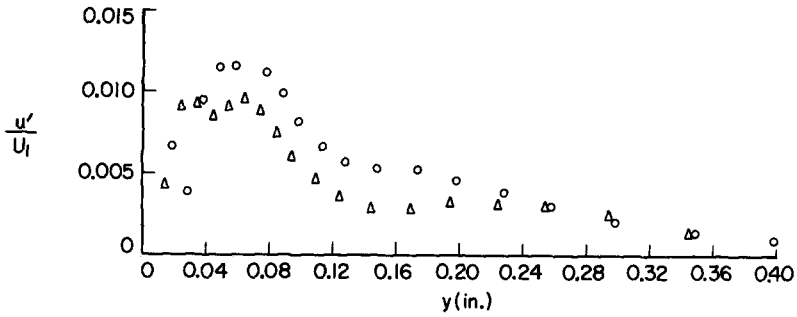

FIG. 8. Intensity of u fluctuation downstream of 0.066-in. diam roughness element at $x_k=2.0$ ft, ⊙ $U_0/\nu=1.67\times 10^5$ (ft^{-1}), $x-x_k=2.0$ in., △ $U_0/\nu=1.42\times 10^5$ (ft^{-1}), $x-x_k=3.0$ in.

where $x_t-x_k=9.0$ in., and transition is closer to the roughness. At 0.5 in. from the roughness the over-all character of the spectrum is the same as that for the lower Reynolds numbers except that the band at the higher frequency end has shifted to higher frequencies with a maximum at about 260 Hz. At 3 in. from the roughness the higher frequencies have undergone damping but at 4.5 in. the behavior has reversed itself with an increase in amplitude of the higher frequencies which continues to increase farther downstream. A reasonable explanation is that this is a manifestation of nonlinear behavior. At the end of the recovery zone, in contrast to that at the lower Reynolds number where a dominant frequency emerged within the Tollmien–Schlichting zone of instability, there is a range of frequencies present. This behavior is apparently governed by the initial disturbance spectrum and the manner in which the various frequencies are amplified.

Thus, it is evident that basically one is dealing with an instability problem within the recovery zone, and that this region is considerably more unstable than the Blasius flow. In order to better understand the nature of this instability, the manner in which the intensity varied in a downstream direction for a number of frequencies over the spectral range was measured in greater detail. Figure 6 shows the growth and decay of various frequencies for Reynolds numbers per ft of 1×10^5, and 1.16×10^5. At the lower unit Reynolds number the beginning of transition was 48 in. downstream from the roughness. The intensity of a given frequency is plotted relative to its intensity, $u_0'(n)$ at 0.5 in. from the roughness. It is seen that, at a constant unit Reynolds number, frequencies grow and damp within the recovery zone, and the neutral position, i.e., the position at which there is no change in intensity, shifts in a downstream direction with decreasing fre-

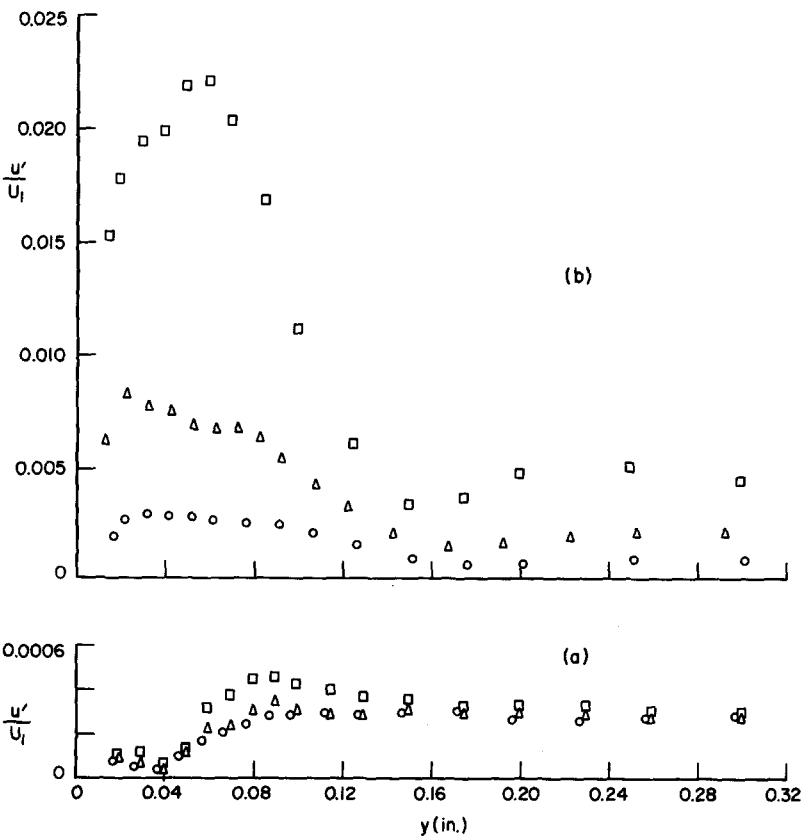

FIG. 9. Intensity of u fluctuation downstream of 0.066-in. diam roughness element at $x_k=2.0$ ft, illustrating increase in amplification within recovery zone. ⊙ $U_0/\nu=1.0\times 10^5$ (ft^{-1}), △ $U_0/\nu=1.16\times 10^5$ (ft^{-1}), ⊡ $U_0/\nu=1.42\times 10^5$ (ft^{-1}). (a) $x-x_k=0.5$ in. (b) $x-x_k=4.5$ in.

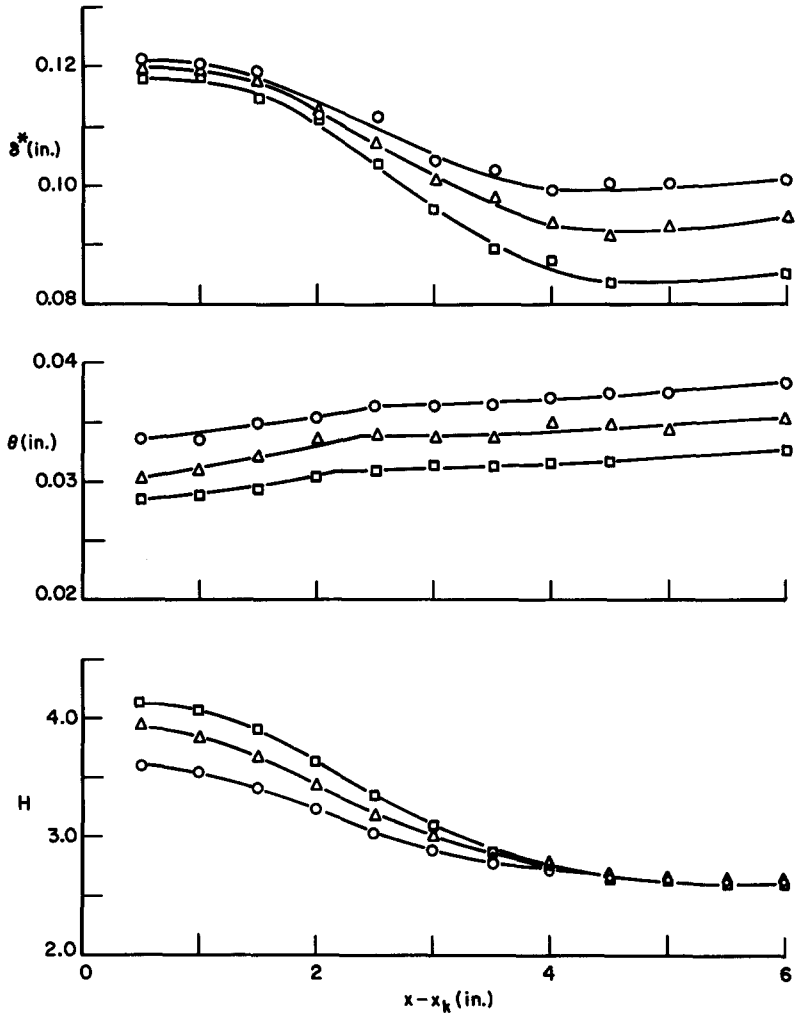

FIG. 10. Distribution of boundary-layer parameters downstream of 0.066-in. diam roughness element at $x_k=2.0$ ft. ⊙ $U_0/\nu=1.0\times10^5$ (ft^{-1}); △ $U_0/\nu=1.16\times10^5$ (ft^{-1}); ⊡ $U_0/\nu=1.42\times10^5$ (ft^{-1}).

quency. The measurements were made at a constant distance of 0.06 in. from the surface; however, measurements across the boundary layer in the vicinity of the neutral position showed that this had no significant effect on the neutral position. With increasing unit Reynolds number the same neutral position is exhibited by a higher frequency. For example, at a unit Reynolds number of 1×10^5(ft^{-1}) the velocity fluctuation with a frequency of 200 Hz is damped at the outset, while at the higher Reynolds number it amplifies over a short distance, has a neutral position at 1.0 in. from the roughness and then damps. Figure 7 shows similar measurements made at two higher Reynolds numbers per foot of 1.42×10^5 and 1.67×10^5. They show the same behavior except that the higher frequencies are considerably more amplified than at the lower Reynolds numbers. For example, at a unit Reynolds number of 1.67×10^5 (ft^{-1}) where transition occurs at 3.0 in. from the roughness, the velocity fluctuation with a frequency of 200 Hz shows no evidence of damping before transition occurs. They also illustrate the behavior referred to earlier, that the higher frequencies, after having undergone some damping, increase in amplitude again. In support of the explanation that this is probably the manifestation of nonlinear behavior is the fact that the maximum over-all intensity of the fluctuation in the boundary layer at the downstream position where the increase occurs, as shown in Fig. 8, is approximately the same, being on the order of one percent. This is consistent with previous observations of the onset of nonlinear behavior with fluctuations introduced by a vibrating ribbon.[5,8]

Although measurements at a constant distance from the surface may introduce a bias in the amplification rates, the curves shown in Figs. 6 and 7 illustrate the general behavior of the amplification. This behavior is consistent with the spectral observations in the immediate downstream vicinity of the roughness, and the shift to higher and higher frequencies with increasing Reynolds number. Frequencies that are unstable in a Blasius flow do not damp, and undergo a very large increase in amplification within the recovery zone. The very large increase in amplification that fluctuations undergo within the recovery zone for a given roughness element, and its dependence on Reynolds number per foot, is illustrated in Fig. 9 which compares the distribution of over-all intensity of fluctuations within the boundary layer at $x-x_k=0.5$ in. with that at $x-x_k=$

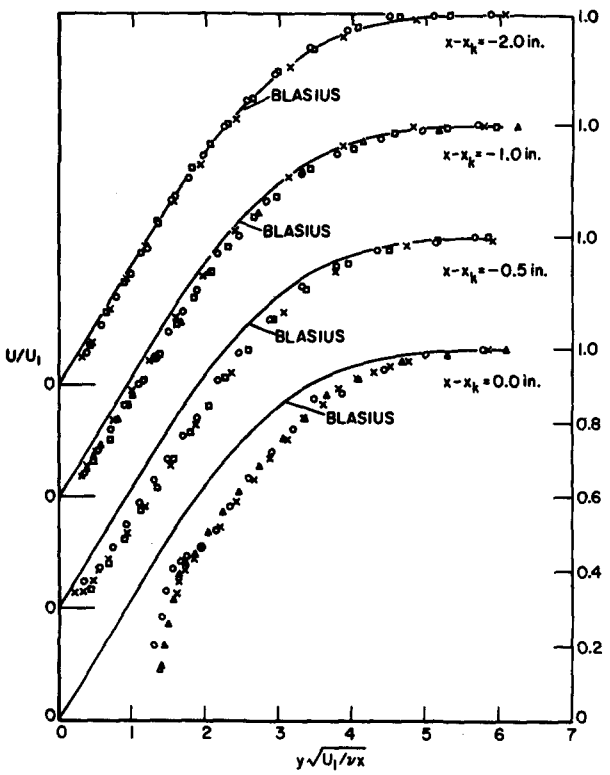

FIG. 11. Mean-velocity distributions at and upstream of 0.066-in. diam roughness element at $x_k=2.0$ ft; ⊙ $U_0/\nu=1.0\times10^5$ (ft^{-1}); △ $U_0/\nu=1.16\times10^5$ (ft^{-1}); ⊡ $U_0/\nu=1.42\times10^5$ (ft^{-1}); × $U_0/\nu=1.56\times10^5$ (ft^{-1}).

4.5 in., the recovery position. It is seen that the maximum over-all intensity increases by factors of approximately 50, 20, and 10, at Reynolds numbers per ft of 1.42×10^5, 1.16×10^5, and 1.0×10^5, respectively.

These results also demonstrate that the basic mechanism by which a two-dimensional roughness element induces earlier transition is essentially the same whether transition occurs within the recovery zone or at a considerable distance downstream. In fact, the "spikes" which characterize breakdown were also observed to occur at a unit Reynolds number of 1.67×10^5(ft^{-1}) with transition occurring at 3.0 in. downstream from the roughness. In this case it should be noted that the position of transition was taken as being the position where the "spikes" were first observed to occur.

IV. MEAN FLOW

It is apparent from the foregoing behavior that as they travel downstream the disturbances pass through a region which is not only more unstable than the Blasius flow but one in which the flow is continuously changing from a very unstable one to the relatively more stable Blasius flow. It is well known that the stability of a flow is primarily dependent on the mean-velocity distribution, and it appears that the explanation lies with the mean-velocity profiles within the recovery zone which change from an initial inflectional type profile to a Blasius profile.

TABLE I. Boundary-layer parameters measured downstream of two-dimensional cylindrical roughness elements.

$x-x_k$ (in.)	δ^* (in.)	θ (in.)	H	k (in.)	x_k (ft)	U_1 (ft/sec)	k/δ_k^*
0.25	0.0896	0.0271	3.31				
0.50	0.0929	0.0287	3.24				
0.75	0.0857	0.0273	3.14				
1.00	0.0870	0.0292	2.98				
1.25	0.0816	0.0273	2.99				
1.50	0.0839	0.0295	2.84	0.043	2.0	23.3	0.56
1.75	0.0814	0.0293	2.78				
2.00	0.0841	0.0308	2.73				
2.25	0.0770	0.0292	2.64				
2.50	0.0757	0.0286	2.65				
2.75	0.0773	0.0299	2.59				
3.00	0.0756	0.0292	2.59				
0.5	0.1358	0.0426	3.19				
1.0	0.1375	0.0441	3.12				
1.5	0.1386	0.0473	2.93				
2.0	0.1341	0.0473	2.83				
2.5	0.1298	0.0472	2.75	0.066	2.0	9.9	0.56
3.0	0.1277	0.0474	2.69				
3.5	0.1272	0.0496	2.56				
4.0	0.1243	0.0477	2.61				
4.5	0.1263	0.0494	2.56				
0.5	0.1472	0.0413	3.56				
1.0	0.1464	0.0422	3.47				
1.5	0.1453	0.0434	3.35				
2.0	0.1414	0.0449	3.15				
2.5	0.1398	0.0464	3.01	0.066	4.58	24.1	0.56
3.0	0.1317	0.0469	2.81				
3.5	0.1270	0.0461	2.75				
4.0	0.1258	0.0469	2.68				
4.5	0.1253	0.0475	2.64				
0.5	0.1561	0.0430	3.63				
1.0	0.1497	0.0433	3.46				
1.5	0.1533	0.0438	3.50				
2.0	0.1453	0.0443	3.28	0.066	5.5	28.2	0.57
2.5	0.1398	0.0441	3.17				
3.0	0.1369	0.0466	2.94				
3.5	0.1313	0.0461	2.85				
4.0	0.1301	0.0471	2.76				
0.5	0.1917	0.0564	3.40				
1.0	0.1887	0.0572	3.30				
2.0	0.1917	0.0596	3.22				
3.0	0.1794	0.0612	2.93	0.088	5.5	15.7	0.56
4.0	0.1749	0.0615	2.84				
5.0	0.1662	0.0614	2.71				
6.0	0.1666	0.0637	2.61				

In order to characterize the mean-velocity profiles within the recovery zone, the customary shape parameter H is used, where H is the ratio of the displacement thickness δ^*, to the momentum thickness θ. The manner in which δ^*, θ, and H vary with distance downstream of the roughness element is shown in Fig. 10 for the three different unit Reynolds numbers at which detailed measurements of the fluctuations were made. The values

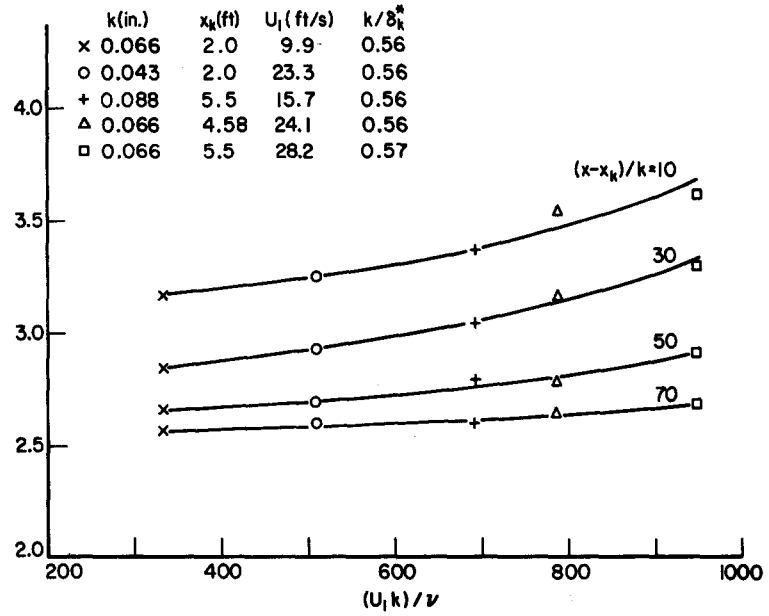

FIG. 12. Variation of shape parameter H with roughness Reynolds number for varying roughness size and position at a fixed value of k/δ_k^*.

of H shown were obtained from the faired data of δ^* and θ, and change from a relatively high value associated with the separated laminar layer to the Blasius value of 2.6 at the recovery position. At approximately 4.5 in. or 70-diam downstream from the roughness element the boundary layer has a velocity profile and growth which are characteristic of a boundary layer without roughness. The kink in the curves of θ reflects the downstream extent of the actual flow separation within the recovery zone with the kink apparently indicating the end of the separated region. The extent of the separated region varies within the range of 30 to 40 roughness diameters and exhibits some dependence on unit Reynolds number. However, the change is small and the range of parameters is too limited to adequately assess this behavior. The shape of the velocity profile in the separated region close to the roughness does show some change with unit Reynolds number. The profiles are less inflectional with decreasing unit Reynolds number and this change in shape no doubt affects the stability. The extent of the recovery zone also appears rather insensitive to the narrow range of unit Reynolds numbers investigated. It is reasonable to expect that the actual extent of the recovery zone will vary not only with roughness size, but for a given roughness element will probably also be observed to vary if a much wider range of unit Reynolds numbers were covered than that shown in Fig. 10. It may well be, therefore, that at considerably lower unit Reynolds numbers, the flow will not only be relatively less unstable but the extent of the destabilizing zone will have decreased.

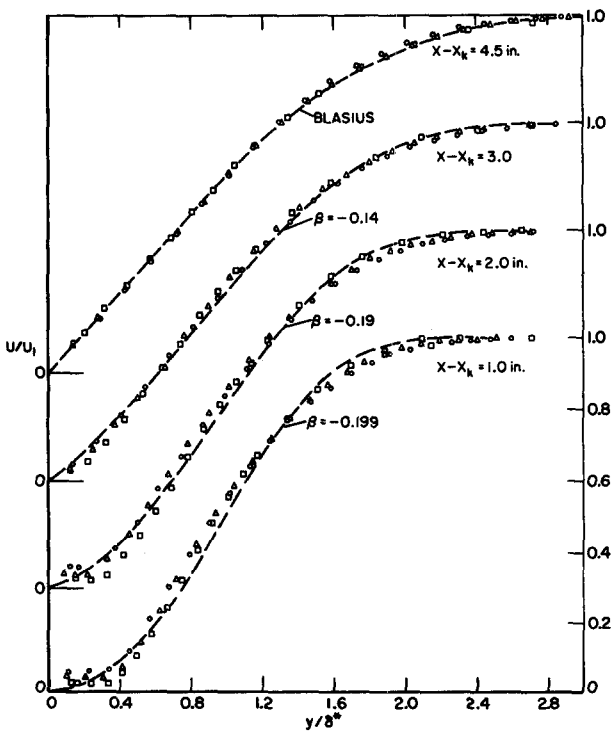

FIG. 13. Mean-velocity distributions downstream of 0.066-in. diam roughness element at x_k=2.0 ft compared with Hartree profiles; ⊙ U_0/ν=1.0×10^6 (ft^{-1}); △ U_0/ν=1.16×10^6 (ft^{-1}); □ U_0/ν=1.42×10^6 (ft^{-1}).

In Fig. 11 measurements are shown of the mean-velocity distribution in the immediate upstream vicinity, and directly above the roughness at a number of different unit Reynolds numbers. There is no evidence of an overshoot in the velocity profile above the roughness, as would be inferred from an analogy with potential flow. To the contrary, the distributions show lower velocities than those for the undisturbed flow. The assumption of a local velocity overshoot would, therefore, seem inappropriate for rationalizing the behavior of trip Reynolds numbers. It is interesting to note that the velocity distributions at each position in the upstream zone of influence of the roughness exhibit a greater degree of similarity than they do downstream of the roughness.

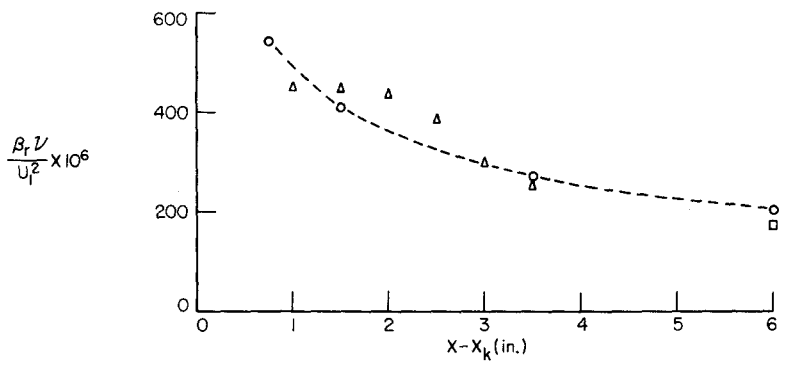

FIG. 14. Comparison of measured neutral frequencies in recovery zone downstream of 0.066-in. diam roughness element at $x_k=2.0$ ft with those obtained from the calculations of Pretsch and Shen. $U_0/\nu=1.16\times10^5$ (ft^{-1}); ○ experimental △ Pretsch; □ Shen.

A change in unit Reynolds number generally incorporates a change in both k/δ_k^*, and the roughness Reynolds number U_1k/ν, and the associated Reynolds number U_kk/ν. In the latter, U_k is the mean velocity that would exist in the boundary layer at the height of the roughness position without the roughness present. It is of interest to examine the dependence of H on these parameters for geometrically similar roughness, particularly from the stability point of view previously alluded to, and the fact that data for the Reynolds number of transition have correlated with k/δ_k^*.[9] Figure 12 shows the variation of H with roughness Reynolds number for two-dimensional cylindrical roughness elements of varying size and at different positions from the leading edge. The conditions were selected so as to maintain the same value of k/δ_k^*. The values of H at the several nondimensional distances downstream from the roughness within the recovery zone were obtained from faired curves through the measured data for H given in Table I. Whereas Fig. 10 incorporates a change in both Reynolds number and k/δ_k^*, Fig. 12 shows only the effect of Reynolds number. Thus, it is seen from comparison of the behavior shown in Figs. 10 and 12 that the shape of the velocity profile and consequently, the stability of the flow, is governed by both k/δ_k^* and the roughness Reynolds number. However, the dependence of the shape of the velocity profile on the latter would appear to be a relatively weak one.

V. INSTABILITY

It is desirable to assess the validity of these conclusions as to the unstable behavior of the recovery zone by making a quantitative comparison with stability theory. Stability calculations available for making such a detailed comparison are those of Pretsch[10] who carried out stability calculations for the Hartree family of profiles using the frictionless perturbation equation. Hartree profiles[11] are solutions of the Falkner and Skan equations for the cases where

$$U_1=\text{const}x^m.$$

The profiles are characterized by the parameter

$$\beta=2m/(m+1),$$

where for decelerated flow $\beta<0$. In the Hartree family of profiles, values of $\beta=-0.199$ and $\beta=0$ correspond to a separation profile and a Blasius profile, respectively.

The shape parameter is a rather poor criterion for assessing the actual inflectional character of the velocity profile. It may well be that the strength of the inflection and its position relative to the surface are the significant criteria and that a parameter involving the derivatives, such as the third derivative, may be more appropriate. However, derivatives obtained graphically are rather inaccurate, and the shape parameter does provide some basis for comparison with inflectional profiles for which a theoretical stability analysis has been carried out. Therefore, the procedure adopted was to select a Hartree profile having the same value of H as the measured profile. Representative mean-velocity distributions for the three unit Reynolds numbers at different positions within the recovery zone are shown in Fig. 13. They are compared at each position, for the purpose of illustration, with a Hartree profile having a value of β corresponding to a shape parameter which is the average of the measured distributions. At $x-x_k=$ 1.0 and 2.0 in. the measurements close to the surface reflect the behavior of a hot wire in a separated region and are consistent with the inference drawn from the θ distributions as to the extent of the separated region. The shape parameters were obtained by extrapolating the distributions smoothly to zero at the surface. There are systematic differences between the distributions at a given position in that they become more inflectional with increasing Reynolds number. At 1 in. downstream from the roughness the measured distributions are somewhat more inflectional than the Hartree profile, with the distribution for the lower Reynolds number in somewhat better agreement. The approximation by a Hartree profile improves in a downstream direction, and at the recovery position there is excellent agreement with the Blasius distribution.

From the stability calculations of Pretsch for flows with different values of β in the range from -0.1 to -0.199, one can estimate for a given β, interpolating where necessary, the neutral frequency at the appropriate boundary-layer Reynolds number $U_1\delta^*/\nu$, for each downstream position within the recovery zone. Figure 14 shows a comparison between these values, and the measured values taken from the growth and

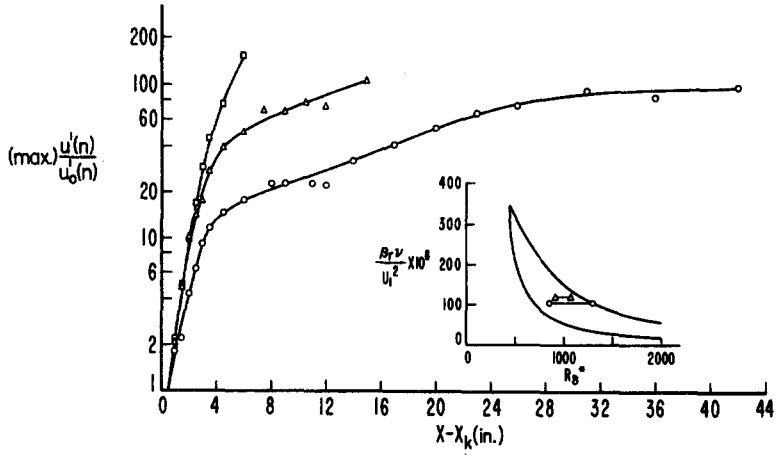

FIG. 15. Growth of selected frequencies downstream of 0.066-in. diam. roughness element at $x_k=2.0$ ft; ○ $U_0/\nu=1.0\times10^6$ (ft^{-1}); $n=29$ Hz, max $u_0'(n)/U_1=0.025\times10^{-3}$; $x_t-x_k=48$ in.; △ $U_0/\nu=1.16\times10^6$ (ft^{-1}); $n=45$ Hz; max $u_0'(n)/U_1=0.039\times10^{-3}$; $x_t-x_k=19$ in.; □ $U_0/\nu=1.42\times10^6$ (ft^{-1}); $n=52$ Hz; max $u_0'(n)/U_1=0.048\times10^{-3}$; $x_t-x_k=9.0$ in.

decay curve shown in Fig. 6 for a Reynolds number of 1.16×10^6(ft^{-1}). The frequency is presented in nondimensional form with $\beta_r=2\pi n$. The measured values are denoted by the open-circle symbols and the dashed curve is drawn through these points primarily for identification, and to indicate the trend. The triangular symbols are the neutral frequencies estimated from the Pretsch calculations, and the square symbol is that obtained from the stability diagram as calculated by Shen for Blasius flow. The latter was used at the end of the recovery zone because of the low accuracy of the Pretsch calculations for Blasius flow where viscous effects are important. Implicit in this comparison is the assumption that what is observed locally is governed by the local mean-velocity distribution. The agreement is fairly good considering the approximate nature of the comparison. A similar comparison was made of the neutral frequencies and their position from the data of Figs. 6 and 7 for Reynolds numbers per ft of 1×10^6 and 1.42×10^6. However, due to the limited extent of these data the comparison is not shown, but it may be said that the agreement was about as good as that shown in Fig. 14.

The agreement of the observed neutral frequencies with the Pretsch calculations was sufficiently encouraging to warrant a quantitative evaluation of the amplification rates which after all is the major consideration in attempting to relate the effect of a roughness element on transition to an instability mechanism. Figure 15 shows the growth of selected frequencies from the immediate downstream vicinity of the roughness to transition at the Reynolds numbers per ft of 1×10^6, 1.16×10^6, and 1.42×10^6. The frequency selected at a particular Reynolds number was one which was domi-

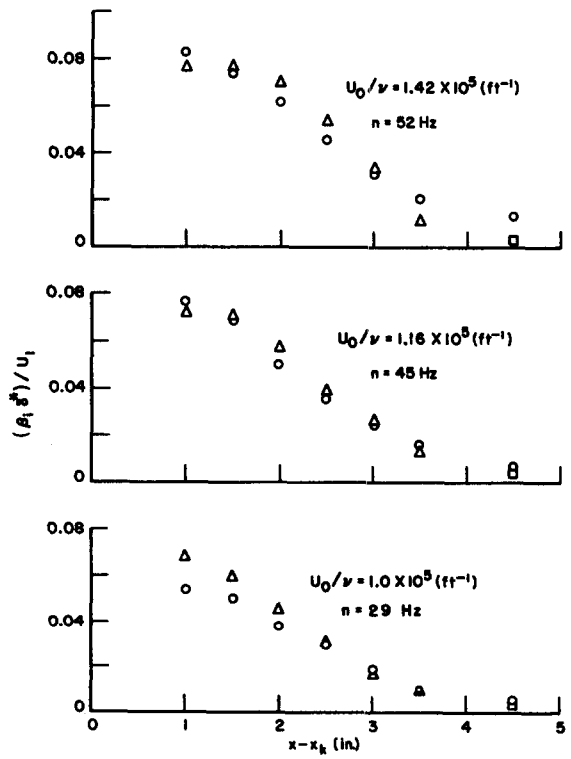

FIG. 16. Comparison of measured amplification rates downstream of 0.066-in. diam. roughness element at $x_k=2.0$ ft with those obtained from the calculations of Pretsch and Shen. ○, experimental; △, Pretsch; □, Shen.

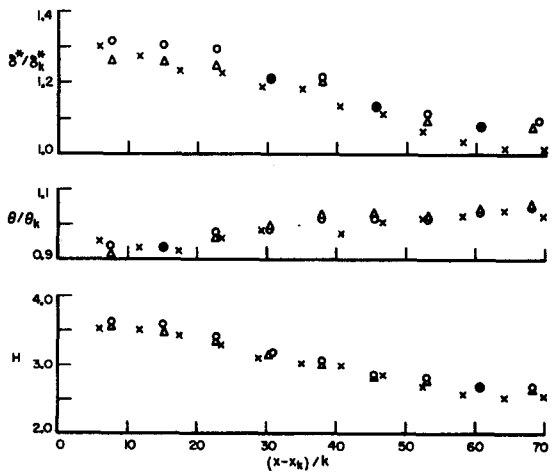

FIG. 17. Distribution of boundary-layer parameters for similar mean flow conditions within the recovery zone. ○ $k=0.66$ in., $x_k=2.0$ ft, $U_0/\nu=1.0\times10^6$ (ft^{-1}); △ $k=0.066$ in., $x_k=4.58$ ft, $U_0/\nu=1.42\times10^6$ (ft^{-1}), × $k=0.043$ in., $x_k=2.0$ ft, $U_0/\nu=2.07\times10^6$ (ft^{-1}).

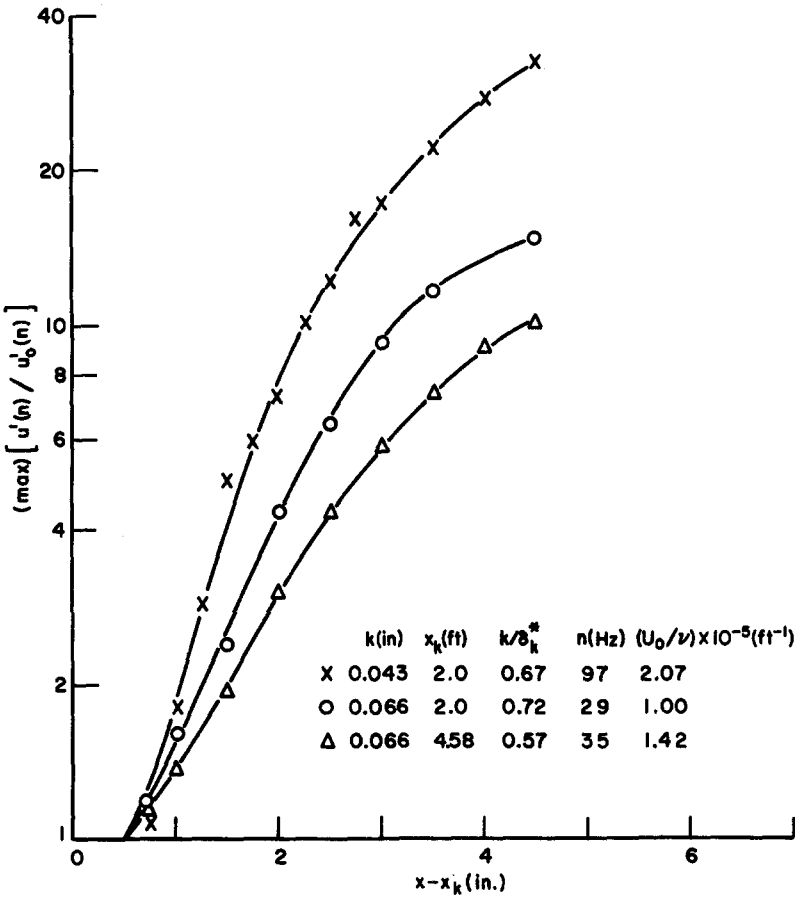

FIG. 18. Amplification of selected frequencies for similar mean flow conditions within the recovery zone. × $u_0'(n)/U_1 = 0.02\times10^{-3}$, ○ $u_0'(n)/U_1 = 0.025\times10^{-3}$, △ $u_0'(n)/U_1 = 0.052\times10^{-3}$.

nant in the spectral distribution of disturbances just prior to transition. When the growth of a disturbance is traced over such a long distance, there is no *a priori* position from the surface, or relative to the boundary-layer thickness which may not bias the amplification rate. The procedure adopted, therefore, was to survey across the boundary layer at each downstream position and to locate the maximum in the intensity. It is this intensity which is shown relative to the initial maximum in intensity at 0.5 in. from the roughness.

The insert in Fig. 15 shows the Tollmien–Schlichting stability diagram as recalculated by Shen, and the points with their connecting lines indicate therein the location of the respective frequencies for the two lower unit Reynolds numbers from the recovery position at 4.5 in. downstream from the roughness to near transi-

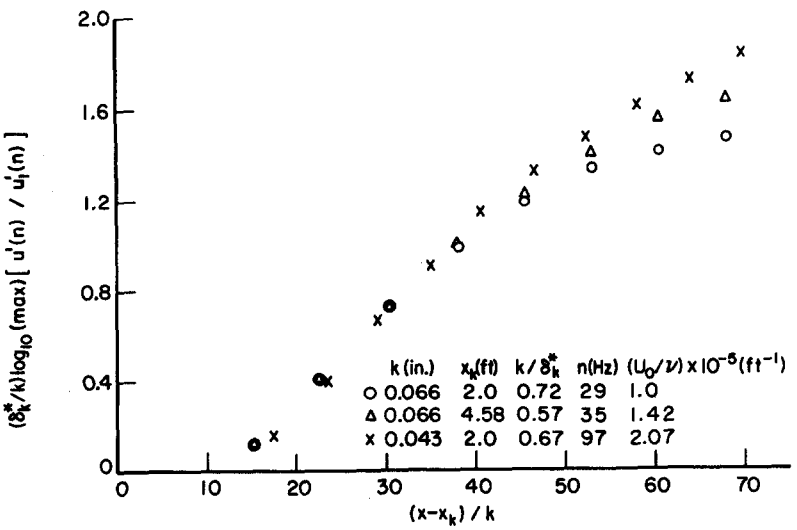

FIG. 19. Correlation of the data of Fig. 18 as suggested by an instability mechanism.

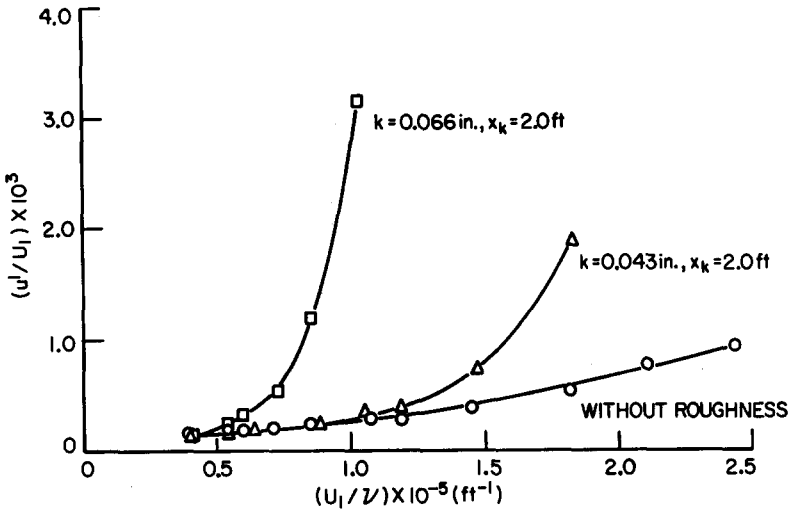

FIG. 20. Comparison of the variation in intensity with unit Reynolds number for roughness with that at the same position without roughness; $x-x_k=4.5$ in., $y=0.06$ in.

tion. The frequency of 45 Hz, at a unit Reynolds number of $1.16\times10^5(ft^{-1})$, extends from about the middle of the diagram to near branch II and, as would be expected in this region, the amplification rate is decreasing. The frequency of 29 Hz, at the lower unit Reynolds number, extends from near branch I to branch II and also exhibits the expected behavior with the amplification rate increasing as it passes through the diagram and decreasing as it approaches branch II. The frequency of 52 Hz, at a unit Reynolds number of $1.42\times10^5(ft^{-1})$, was omitted from the Tollmien–Schlichting stability diagram because of its nonlinear behavior.

Within the recovery zone the amplification rates are much greater than within the region of Blasius flow. A comparison of the nondimensional amplification rates measured within the recovery zone with those calculated by Pretsch using the approximation of a Hartree profile as previously outlined is shown in Fig. 16. The theoretical nondimensional amplification rate at the recovery position was obtained from the Shen calculations for Blasius flow. The amplification rate, β_i, for the different frequencies at the various positions within the recovery zone was obtained by graphical differentiation of the measurements shown in Fig. 15, i.e.,

$$\frac{u'(n)}{u_0'(n)}=\exp\int_{t_1}^{t_2}\beta_i\,dt, \tag{1}$$

and

$$\beta_i=2.3c_r\frac{d\{\log_{10}[u'(n)/u_0'(n)]\}}{dx}. \tag{2}$$

Included in this comparison, therefore, is the additional assumption that the temporal amplification and spatial amplification rates are related by the wave velocity, c_r. The comparison does not merit the refinement of attempting to use the more appropriate group velocity. The values of wave velocity which were used were obtained from the Pretsch calculations. At the unit Reynolds number of $1.42\times10^5(ft^{-1})$ the nonlinear behavior previously alluded to manifests itself near the downstream end of the recovery zone, with an amplification rate at the recovery position approximately four times higher than the theoretical value for Blasius flow. In general, the agreement is better than might have been expected considering not only the approximations and assumptions involved, but also the approximate nature of the theoretical calculations. An indirect result of this comparison as well as that shown in Fig. 14 is the inference that may be drawn in regard to certain aspects of boundary-layer stability theory, namely, the question as to the equivalence of spatial and temporal growth, and the effect of the spatial rate of change of the boundary layer. The results strongly suggest that these are not necessarily serious limitations, particularly when it is considered that the agreement between experiment and theory shown in Figs. 14 and 16 was obtained under conditions where the amplification rates are much greater than in the Blasius flow region and the mean-velocity profile changes rapidly from a separated type to a Blasius profile. The inflections in the experimental mean-velocity profiles are closer to the surface than for the corresponding Hartree profile and would indicate values of wave velocity lower than those obtained from the Pretsch calculations. It may, therefore, also be in order to introduce a word of caution as to any inference that this is a valid test of Pretsch's calculations. The purpose was solely to evaluate whether the effect of a two-dimensional roughness element on boundary-layer transition can be classed as a stability governed phenomenon.

It is possible, however, to provide what may be considered as a self-consistent experimental check on the validity of the stability mechanism outlined above. The amplification given by Eq. (1) can be rewritten in terms of dimensionless quantities.

$$\log\frac{u'(n)}{u_1'(n)}=\frac{k}{\delta_k^*}\int_{(x-x_k/k)_1}^{(x-x_k/k)}\frac{\beta_i\delta^*}{U_1}\frac{U_1}{c_r}\frac{\delta_k^*}{\delta^*}\,d\left(\frac{x-x_k}{k}\right). \tag{3}$$

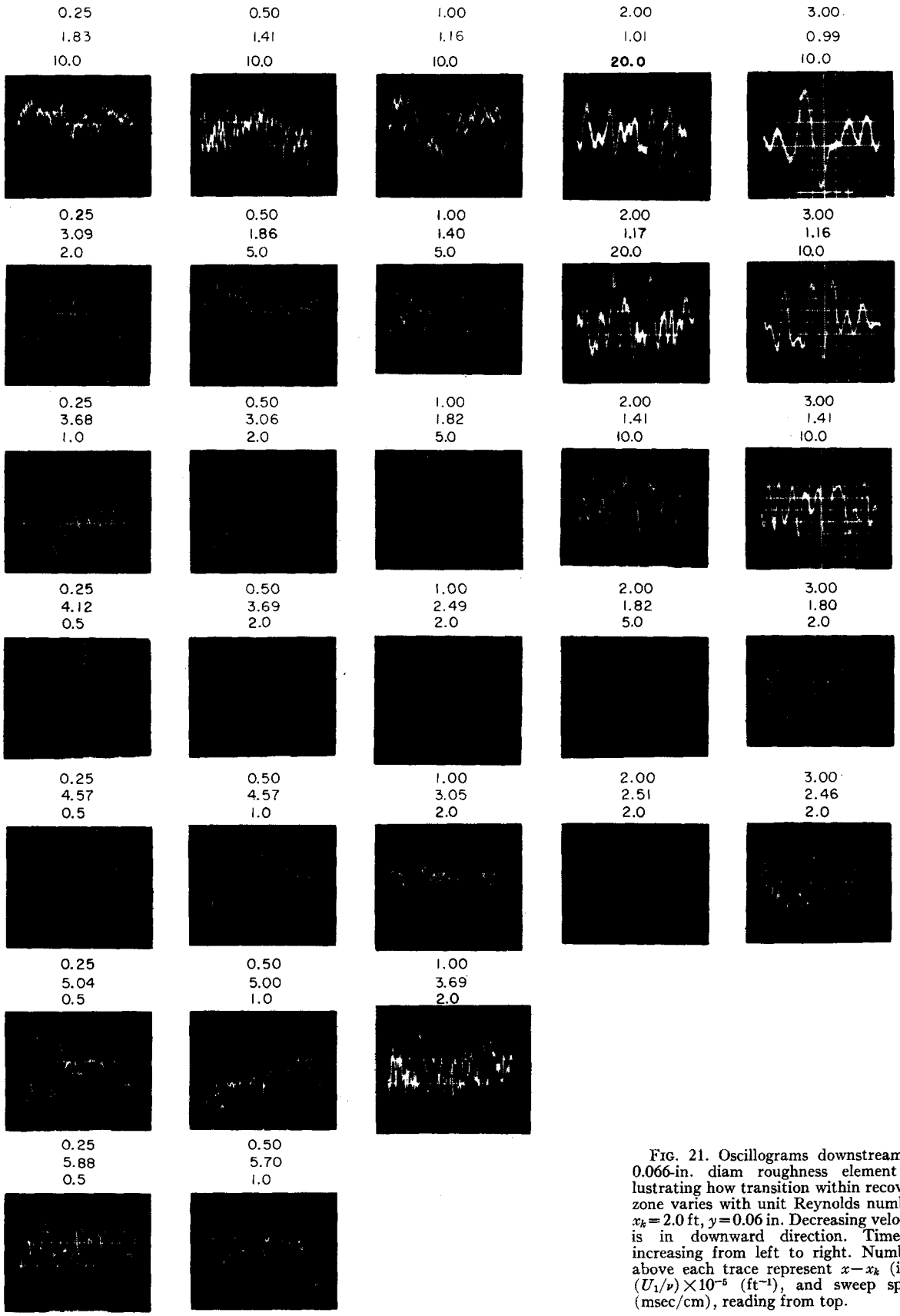

FIG. 21. Oscillograms downstream of 0.066-in. diam roughness element illustrating how transition within recovery zone varies with unit Reynolds number: $x_k = 2.0$ ft, $y = 0.06$ in. Decreasing velocity is in downward direction. Time is increasing from left to right. Numbers above each trace represent $x - x_k$ (in.), $(U_1/\nu) \times 10^{-5}$ (ft^{-1}), and sweep speed (msec/cm), reading from top.

By carefully controlling the experimental conditions, it should be possible to correlate the growth for specific frequencies in a form consistent with Eq. (3). Figure 17 shows the measured distributions of δ^*, θ, and H obtained by experimentally adjusting k/δ_k^*, and U_1k/ν, in order to obtain, for varying roughness size and position, the same distribution of H with $(x-x_k)/k$ within the recovery zone. The nondimensional boundary-layer parameters for the different conditions agree reasonably well for the present purpose. Although the corresponding velocity profiles are not shown, it may be stated that they exhibited a high degree of similarity. Thus, one would expect the distributions of $\beta_i\delta^*/U_1$ with $(x-x_k)/k$ to be similar. Implicit in this comparison is the assumption that the nondimensional amplification rate does not depend on Reynolds number. If the dimensionless wave velocities are also regarded as being similar for the different conditions, which is not an unreasonable assumption, particularly for inflectional profiles, then the growth of specific frequencies should correlate with k/δ_k^*. Figure 18 shows the growth of specific frequencies for the various experimental conditions noted on the figure, which were chosen so as to have approximately the same value of the dimensionless wavenumber $\alpha\delta^*$. The value of $\alpha\delta^*$ chosen was 0.3. According to the Pretsch calculations, the dimensionless amplification rate would not be too sensitive to small deviations from this value. As for the data shown in Fig. 15, the maximum in the distribution of intensity across the boundary layer for a given frequency was used to characterize the behavior. The initial growth of the various frequencies illustrates what appears to be an apparent anomaly; that is, that the maximum gradient does not appear to be at the initial position as one would expect from the instability model presented. The reason for this behavior is not evident but a possible explanation is that the initial behavior is masked by the effect of free-stream disturbances even though the intensity of free-stream distributions for the present investigation is low. Nevertheless, as shown in Fig. 19 with $u_1'(n)$ corresponding to the intensity at the initial position

$$[(x-x_k)/k]_1=11.6,$$

the growth of the various frequencies does correlate reasonably well in accordance with Eq. (3) up to a value of $(x-x_k)/k$ of approximately 40. At this position H is about 3.0, corresponding to relatively weak inflectional profiles. Farther downstream an effect of Reynolds number can be observed.

It may be remarked that the trend with Reynolds number is consistent with the manner in which the various frequencies locate in the instability diagram for Blasius flow. The results are also of interest in regard to the general problem of stability in that it may be inferred that the effect of boundary-layer Reynolds number can be neglected for relatively strong inflectional profiles. This has frequently been assumed in theoretical calculations but had not been observed experimentally.

VI. CRITICAL REYNOLDS NUMBERS

The over-all effect of the recovery zone on fluctuations is illustrated in Fig. 20 in which the variation of u'/U_1, at the end of the recovery zone, is shown for a range of unit Reynolds numbers, and compared with the intensity that would exist at the same position without roughness. The behavior shown is for cylindrical roughness elements 0.066 and 0.043 in. in diameter mounted 2 ft from the leading edge of the flat plate. The measurements were made at a fixed position of the surface, $y=0.06$ in., and at 4.5 in. downstream from the roughness elements. As the Reynolds number decreases the rate of change of intensity becomes less and less, and at a sufficiently low Reynolds number there is no significant amplification by the recovery zone. Reynolds numbers per ft of 0.59×10^5 and 1.04×10^5, for the 0.066- and 0.043-in. diam roughness, respectively, correspond to a roughness Reynolds number U_kk/ν of 100. This behavior is not inconsistent with attempts to specify, from empirical correlations of transition position, a Reynolds number for when a two-dimensional roughness will not affect transition.[12,13] However, there is no evidence that such a Reynolds number is unique in a critical sense. The observed behavior is apparently due not only to the decrease in amplification with decreasing Reynolds number, but also to the fact that at the lower Reynolds numbers the mean flow in the recovery zone is less inflectional and therefore not as unstable. Apparently, any critical flow behavior, as suggested by Schiller and discussed by Goldstein,[14] would reflect itself only indirectly through the change it manifests in the mean-velocity distribution.

Considerable experimental activity has also been directed toward establishing a Reynolds number criterion for when transition would be attached to the roughness. Reasonably good empirical correlation of transition data is obtained for two-dimensional roughness elements as long as the position of transition is downstream from, and not too close to the roughness element. However, as x_t approaches x_k, i.e., $x_t/x_k<1.2$, significant departures from such correlations occur.[9,13] This behavior is consistent with the effect of roughness within the context of an instability mechanism. Figure 21 shows oscillograms of the u fluctuation at $y=0.062$ in. for varying unit Reynolds number, and at different positions in the immediate downstream vicinity of a 0.066-in. diam roughness element mounted at $x_k=2.0$ ft. The distance downstream from the roughness, the unit Reynolds number, and the sweep speed are noted above each oscillogram. As for Fig. 3, no particular significance should be attached to the relative amplitudes of the fluctuations shown in the different oscillograms. The quasiperiodic fluctuations with frequencies decreasing

in the downstream direction, and increasing with unit Reynolds number, as discussed in Sec. III, are shown, as well as the fact that transition within the recovery zone moves forward very slowly with increasing unit Reynolds number. For example, at 1 in. from the roughness there is evidence of the onset of turbulence at a unit Reynolds number of $2.49\times10^5(\text{ft}^{-1})$, while at 0.5 in. from the roughness there is little evidence of turbulence at a unit Reynolds number of $3.06\times10^5(\text{ft}^{-1})$. Reynolds numbers for when transition is attached to the roughness may, therefore, vary widely depending on how precisely the position of attachment is defined, and it is not surprising that attempts to specify a critical Reynolds number for attachment exhibit a great deal of scatter. It may be that some specified criterion for attachment, such as an appropriate extrapolation of transition data to the roughness position,[13] or considering attachment to occur when transition is at the recovery position, may be helpful but the question of uniqueness remains. In view of the instability mechanism the Reynolds number for attachment, unlike the Reynolds number for not affecting transition, will depend on the ambient conditions, and will be subject to the many factors which influence the transition process.

VII. CONCLUDING REMARKS

The experimental evidence would appear to be sufficient for concluding that the effect of a two-dimensional roughness element on boundary-layer transition can be regarded as a stability governed phenomenon. It is not necessarily engaging in semantics to say that the roughness of itself does not introduce disturbances which add to the disturbance level in the boundary layer, but that the basic mechanism by which a two-dimensional roughness element induces earlier transition is by the destabilizing influence of the flow in the recovery zone on existing disturbances which hastens the downstream development of the instability. Depending on the extent of destabilization, this process may occur so quickly that transition will occur close to the element. It is reasonable to draw the conclusion that the character of the instability depends on the nature of the velocity profile generated, and it is in this connection that some influence of the roughness shape may also be expected. Under appropriate conditions of much larger roughness elements than in the present investigation, or if the roughness element is off the surface, the inflectional nature of the velocity profile may be such that the instability will be characteristic of a free-shear layer instability rather than the boundary layer type of instability observed in the present experiment. The fact that the effect of a two-dimensional roughness on transition is a stability governed phenomenon is also consistent with the effect of a two-dimensional roughness at higher Mach numbers and provides an explanation for the difficulty encountered in attempting to trip a boundary layer at high Mach number.

ACKNOWLEDGMENTS

The authors wish to express their gratitude to Mr. L. Sargent for his assistance in the experimental program, and the tabulation and preparation of data.

This work was performed with the support of the Office of Advanced Research and Technology, National Aeronautics and Space Administration, Order No. W 13-147.

[1] H. W. Liepmann, NACA Wartime Report, ACR 3H30 (1943).
[2] P. S. Klebanoff, G. B. Schubauer, and K. D. Tidstrom, J. Aeron. Sci. **22**, 803 (1955).
[3] I. Tani and H. Sato, J. Phys. Soc. Japan **11**, 1284 (1956).
[4] M. V. Morkovin, Trans. ASME **80**, 1121 (1958).
[5] P. S. Klebanoff, K. D. Tidstrom, and L. M. Sargent, J. Fluid Mech. **12**, 1 (1962).
[6] L. S. G. Kovasznay, H. Komoda, and B. R. Vasudeva, in *Proceedings of the 1962 Heat Transfer and Fluid Mechanics Institute* (Stanford University Press, Stanford, California, 1962), p. 1.
[7] S. F. Shen, J. Aeron. Sci. **21**, 62 (1954).
[8] P. S. Klebanoff and K. D. Tidstrom, NASA Technical Note D-195 (1959).
[9] I. Tani, in *Boundary Layer and Flow Control*, edited by G. V. Lachmann (Pergamon, New York, 1961), Vol. 2, p. 637.
[10] J. Pretsch, NACA Technical Memorandum 1343 (1952).
[11] D. R. Hartree, Proc. Cambridge Phil. Soc. **33**, 223 (1937).
[12] A. M. O. Smith and D. W. Clutter, J. Aerospace Sci. **26**, 229 (1959).
[13] J. C. Gibbings, Aeron. Res. Council (Great Britain) Tech. Rept. No. 462 (1959).
[14] S. Goldstein, Aeron. Res. Comm. (Great Britian) Rept. Mem. No. 1763 (1936).